

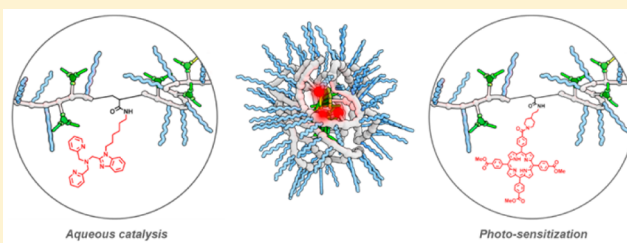
Modular Synthetic Platform for the Construction of Functional Single-Chain Polymeric Nanoparticles: From Aqueous Catalysis to Photosensitization

Yiliu Liu,[†] Thomas Pauloehrl,[†] Stanislav I. Presolski, Lorenzo Albertazzi, Anja R. A. Palmans,* and E. W. Meijer*

Institute for Complex Molecular Systems, Laboratory of Macromolecular and Organic Chemistry, Eindhoven University of Technology, P.O. Box 513, 5600 MB, Eindhoven, The Netherlands

S Supporting Information

ABSTRACT: Single-chain polymeric nanoparticles (SCPNs) are intriguing systems for multiple applications. In order to arrive at a controlled, but random, positioning of the different side groups to the polymer backbone, alternative synthetic routes have to be developed. Here, a general postpolymerization modification strategy of poly(pentafluorophenyl acrylate) (pPFPA) is presented as a versatile method to rapidly access functional SCPNs. We first show that the sequential addition of a benzene-1,3,5-tricarboxamide-based amine, acting as the supramolecular recognition motif, and water-soluble polyetheramine (Jeffamine) to pPFPA affords random copolymers that fold in water into SCPNs. The scope of the modular platform is illustrated by preparing two types of functional SCPNs. First, we prepared SCPNs designed for bio-orthogonal catalysis by attaching pendant mono(benzimidazolymethyl)-bis(pyridylmethyl) (Bimpy), phenanthroline (Phen), or 2,2'-bipyridine (BiPy), ligands capable of binding either Cu(I) or Pd(II). The Bimpy- and Phen-containing SCPNs ligated to Cu(I) significantly accelerate azide–alkyne cycloaddition reactions while Bimpy-containing SCPNs ligated to Pd(II) efficiently catalyze depropargylation reactions. In all cases, reactions proceeded efficiently in phosphate buffer at a physiological pH and at low substrate concentrations. Next, the potential of SCPNs for photodynamic therapy was evaluated. Introducing porphyrins in SCPNs leads to novel photosensitizers that can produce singlet oxygen ($^1\text{O}_2$) upon photoirradiation. Additionally, by attaching both porphyrins and prodrug models, attached via $^1\text{O}_2$ -cleavable amino-acrylate linker, to the SCPNs, we show that irradiation of the SCPNs results in a cascade reaction of $^1\text{O}_2$ generation followed by cleavage of the amino-acrylate linkers, releasing the drug model. The modular synthesis strategy reported here provides rapid and controlled access to SCPNs with tunable amounts of active units that fulfill different functions.



INTRODUCTION

Inspired by nature, numerous efforts have been undertaken to control the three-dimensional structure of synthetic macromolecules and thereby broaden their scope for potential applications. Macromolecular architectures with predefined conformations, such as dendrimers, helical polymers, and star polymers, show improved performance in (asymmetric) catalysis, light harvesting, and sensing.¹ Folding of a single linear polymer chain into a single-chain polymeric nanoparticle (SCPN), which is reminiscent of the folding of proteins, has recently been realized as an alternative approach for the construction of proteinlike functional objects.² Our group focuses on supramolecular folding of single-chain polymers by applying either benzene-1,3,5-tricarboxamide (BTA) or 2-ureido-4[1H]-pyrimidinone (UPy) moieties as supramolecular recognition motifs.³ In particular, water-soluble SCPNs with a compartmentalized hydrophobic interior are obtained by introducing oligo(ethylene glycol) (oEG) as side chains and employing BTAs as supramolecular structuring motifs.^{3d–g} Introducing catalytic sites into these SCPNs has resulted in

efficient catalysis in water owing to the isolation of catalytic sites in the hydrophobic compartments.^{3e,f}

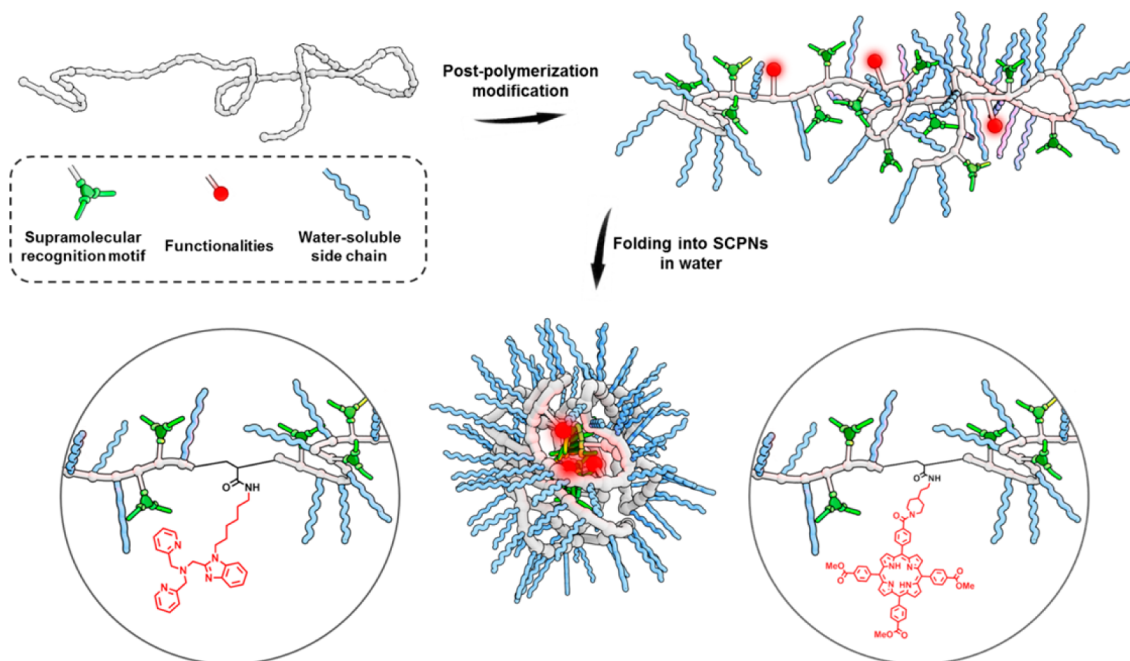
Here, we expand and evolve our SCPN platform by developing new water-soluble SCPNs that exhibit carefully designed functions, with the aim to advance SCPNs to function in complex media. We have particularly been intrigued by the recent development of highly efficient and selective bio-orthogonal, catalytic reactions that permit to manipulate and modify biomolecules within their native cellular conditions⁴ and the advancements in photodynamic therapy (PDT).⁵ A well-known example of a bio-orthogonal reaction is the Cu(I)-catalyzed azide–alkyne cycloaddition (CuAAC),⁶ which has been explored in a cellular context,⁷ and it is found that the toxicity of Cu ions needs to be taken into account.^{8,9} In addition, Pd-catalyzed reactions have recently been applied in living cells.¹⁰ Apart from the possibilities that bio-orthogonal reactions offer, PDT, a nonsurgical method for the localized

Received: August 6, 2015

Published: September 21, 2015



Scheme 1. Representation of Polymers with Different, Pendant Functionalities and Their Folding into Single-Chain Polymeric Nanoparticles in Aqueous Solution



treatment of cancers, is also a highly interesting application. The localization of photosensitizers in tumor sites followed by activation of photosensitizers with light irradiation generates reactive oxygen species (ROS, e.g., $^1\text{O}_2$) to induce cellular damage and destroy tumors. Porphyrins, for example, show effective energy absorption and high $^1\text{O}_2$ quantum yields, making them appealing as photosensitizers.¹¹ However, because of their large π -surface, they are poorly water-soluble and easily form aggregates by hydrophobic and π -stacking interactions, which leads to self-quenching of the excited states and thus lower the photodynamic efficiency.¹²

The SCPN approach is proposed to be advantageous for both types of envisaged applications because SCPNs not only show good water-solubility, but also possess a compartmentalized structure which allows site isolation. These features are highly reminiscent of those contributing to the effectiveness of enzymes¹³ or the porphyrin-containing hemeprotein. The unique structural features of these natural biomacromolecules inspired us to design ligand-containing SCPNs that bind to transition metal catalysts, such as Cu and Pd, to develop biocompatible organometallic catalysts. In addition, the structural characteristics of SCPNs are ideal for isolating pendant porphyrin moieties, hereby enhancing their photosensitizer capabilities. Ideally, the oEG shell of SCPNs will endow SCPNs with optimal pharmacokinetics/circulation half-life as well as tolerance toward enzymatic degradation in living organisms.

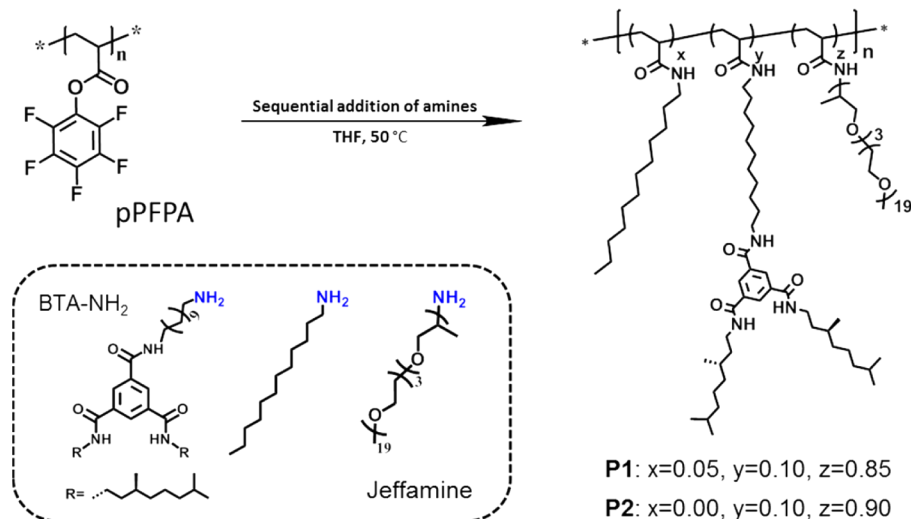
The preparation of SCPNs with tailored functionalities requires combinations of different, and also more complex, monomers. The use of such functional monomers in controlled polymerizations have the danger, however, to result in poorly controlled compositions of the copolymers and/or a loss of control during radical polymerization process.^{3e} As an alternative, a postpolymerization modification strategy may offer a solution for these issues.¹⁴ In this context, polymers with reactive ester side groups that readily react with amines attracted our interest.^{15–18} In fact, poly(pentafluorophenyl

acrylate) (pPFPA), as introduced by Theato et al., is conveniently synthesized by reversible addition–fragmentation chain-transfer polymerization (RAFT) and shows high reactivity toward amines in comparison to its *N*-hydroxysuccinimide (NHS) analogues.¹⁹ In addition, it proved a successful approach for chemically cross-linking single polymer chains.^{19f,g}

Here we report the use of postpolymerization modification as a modular synthetic strategy to prepare multifunctional amphiphilic copolymers that fold into SCPNs (Scheme 1). By reacting the easily accessible amines of water-soluble polyetheramines (Jeffamine), supramolecular recognition units (BTA-NH₂) and the required functionalities with precursor polymers that bear activated esters, multifunctional copolymers become accessible in a controlled manner. The copolymers formed are designed to fold into SCPNs in aqueous solution, a process driven by the triple hydrogen-bonding between the BTA motifs. By employing this synthetic strategy, two types of functional SCPNs, that is, SCPN-based bio-orthogonal organometallic catalysts, and photosensitizer prodrugs, were straightforwardly prepared and their full characterization and catalytic/photosensitizing properties are reported here.

RESULTS AND DISCUSSION

Synthesis of SCPNs by Postpolymerization Modification. Poly(pentafluorophenyl acrylate) homopolymer (pPFPA₁₀₀, $M_{n,SEC} = 14.8$ kDa, $\bar{D} = 1.19$, DP = 100) was synthesized by RAFT polymerization in the presence of 4-cyano-4-(phenylcarbonothioylthio)pentanoic acid as chain transfer agent. Then, polymer analogous reactions were initiated by the sequential addition of amines. This enabled the stepwise functionalization of the polymeric backbone with systematic control over the side chain densities. In order to incorporate the supramolecular recognition motif and water-soluble side chains, the enantiomerically pure, amino-functionalized BTA unit (BTA-NH₂) and Jeffamine M-1000 (a commercially available and hydrophilic polyether monoamine)

Scheme 2. Synthesis of P1 and P2 by Post-Polymerization Modification of pPFPA₁₀₀

were employed. As a proof of principle, polymers P1 (10% BTA-NH₂, 5% dodecylamine, and 85% Jeffamine) and P2 (10% BTA-NH₂ and 90% Jeffamine) were synthesized (Scheme 2). The functionalization of the precursor pPFPA₁₀₀ was followed by ¹⁹F-NMR, a particularly useful tool to monitor the reaction progress (Figure 1a). A ¹⁹F NMR spectroscopic measurement of the reaction mixture was performed after each amine addition step. The conversion was determined by comparing the signal of released pentafluorophenol to the broad fluorine signals of pPFPA₁₀₀ precursor. The conversions determined via ¹⁹F NMR analysis were in full agreement with the targeted polymer composition and the final polymers were obtained after removal of the pentafluorophenol byproduct via dialysis. The FT-IR spectra of P1 and P2 show the characteristic amide band at 1650 cm⁻¹ (CO stretch) and no remaining signal of the carbonyl signal of the activated ester at 1780 cm⁻¹ (Figure 1b). The size exclusion chromatography (SEC) traces of both P1 and P2 measured in DMF reveal that the molar mass dispersity of both polymers remained narrow after the polymer analogous reaction (Table 1, Figure 1c, $\mathcal{D} = 1.16$ for P1 and 1.15 for P2).

Folding of P1 and P2 into SCPNs. In a previous study, we prepared amphiphilic BTA based-polymers^{3d} using the polymerization of methacrylate monomers, whereas here we prepare polyacrylamide-based polymers. In addition, we introduce Jeffamine-based side chains. It is therefore important to first assess in how far these changes in the polymer structure affect the ability of the amphiphilic polymers to form SCPNs. The BTA moieties are expected to form stacked aggregates through triple hydrogen-bonding, thus folding the polymers into compact conformations. This process is easy to follow using a combination of circular dichroism (CD) spectroscopy and dynamic light scattering (DLS).^{3d,g}

P1 and P2 show excellent solubility in water, likely the result of the long, hydrophilic Jeffamine-based side chains of the polymers. The CD spectra of P1 and P2 show negative Cotton effects at 223 nm, which indicates that the BTAs form aggregates with a preferred left-handed (*M*) helical sense (Figure 2a,b). The size of the Cotton effect is slightly higher in P1 ($\Delta\epsilon = -28 \text{ L mol}^{-1} \text{ cm}^{-1}$) than in P2 ($\Delta\epsilon = -22 \text{ L mol}^{-1} \text{ cm}^{-1}$), suggesting that the introduction of additional hydrophobic dodecyl side chains in P1 enhances the BTA stacking.^{3d} In addition, the intensity of the CD effect decreases with

increasing temperature, and almost disappears at 90 °C. Upon cooling the solution, the CD signal increases in size again. The heating and cooling processes show no hysteresis, indicating that these systems are in thermodynamic equilibrium (Figure S6).

These results indicate that the polymers fold and unfold reversibly by controlling the temperature due to the dynamic nature of the hydrogen bonds. In addition, the size of the molar ellipticity $\Delta\epsilon$ in P2 is similar to our previously studied systems ($\Delta\epsilon = -13$ to $-19 \text{ L mol}^{-1} \text{ cm}^{-1}$) showing that the poly(acrylamide)-based backbone and longer Jeffamine-based side chains do not hamper the BTA's aggregation. From the DLS measurements in water (Figure 2c,d), we can extract a hydrodynamic radius R_h of approximately 8.2 and 7.4 nm for P1 and P2, respectively. These values are consistent with those of a polymer that adopts a single-chain folded conformation in solution.^{3d-g}

The post-polymerization modification of pPFPA provides a simple and modular synthetic access to polymers that fold into SCPNs. With this versatile strategy, we continued to synthesize polymers with different functionalities, with the aim to prepare SCPNs that exhibit a function.

Modular Synthetic Platform for Functional SCPNs.

Following the procedure developed for P1 and P2, we first synthesized a series of ligand-containing polymers for preparing catalytically active SCPNs (Figure 3a). In these polymers, different nitrogen-containing ligands, mono-(benzimidazolymethyl)-bis(pyridylmethyl) amine (Bimpy), phenanthroline (Phen), and 2,2'-bipyridine (Bipy), were introduced along with the BTA motifs and Jeffamine-based side chains. Among them, Bimpy and Phen are well-known Cu(I)-binding ligands with CuAAC acceleration properties,²⁰ whereas Bipy coordinates with Pd(II) ions.²¹ Ligands with amine moieties, Bimpy-NH₂ and Bipy-NH₂, were synthesized following literature procedures²² while Phen-NH₂ was commercially available. By employing the post-polymerization modification of pPFPA with ligand-NH₂, BTA-NH₂ and Jeffamine, P3–P5 were obtained in a straightforward fashion. To illustrate the versatility of this approach for accessing multifunctional polymers, the ¹⁹F NMR spectra of the postfunctionalization of pPFPA₁₀₀ with BTA-NH₂, Bipy-NH₂, and Jeffamine, respectively, to afford P5 are shown in Figure 3b.

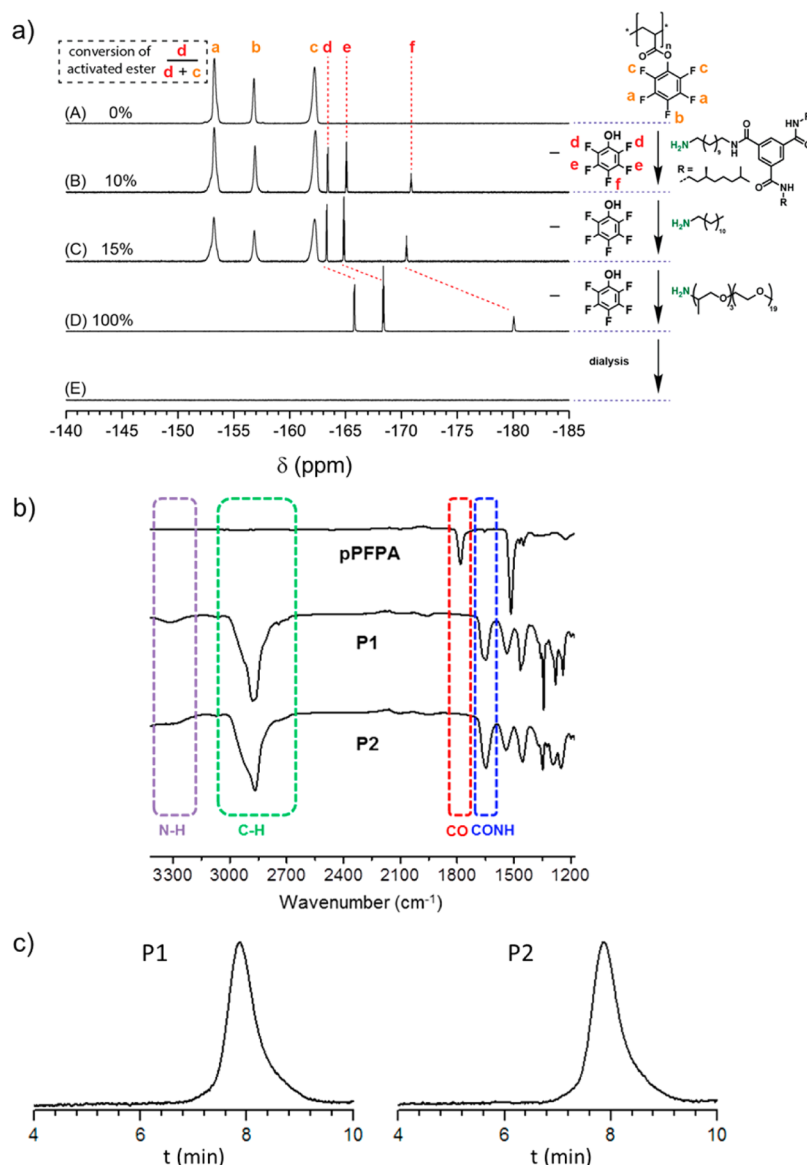


Figure 1. (a) ^{19}F NMR spectra in CDCl_3 of pPFPA₁₀₀ (A) and its sequential modification with BTA-NH₂ (B), dodecylamine (C), and Jeffamine (D) to prepare P1 in which no ^{19}F is present after dialysis (E). (b) FT-IR spectra of pPFPA₁₀₀ and polymers P1 and P2 measured in the bulk. (c) SEC traces of P1 and P2 measured in DMF with 10 mM LiBr, relative to poly(ethylene oxide) standards.

Table 1. Characterization of the Precursor Polymer pPFPA₁₀₀ and P1, P2 by SEC and DLS

polymer	$M_{n,\text{SEC}}$ [kDa] ^a	D [-] ^a	R_h [nm] ^b	DP [-] ^c	$M_{n,\text{ca.}}$ [kDa] ^d
pPFPA ₁₀₀	14.8	1.19		100	24.1
P1	28.1	1.16	8.2	100	101.4
P2	28.9	1.15	7.4	100	105.7

^apPFPA₁₀₀ was measured in THF, relative to polystyrene standards; P1 and P2 were measured in DMF with 10 mM LiBr, relative to poly(ethylene oxide) standards. ^bHydrodynamic radius as determined by DLS. ^cDegree of polymerization (DP) was calculated from the monomer PFPA conversion by NMR to prepare precursor polymer pPFPA. ^dCalculated molecular weight derived from the DP.

Moreover, we prepared a series of polymers that show photosensitizing properties (Figure 4). This was enabled by our previous work on the facile and scalable synthesis of a porphyrin derivative with a single reactive carboxylic acid handle.²³ In P6, porphyrins are attached as photoactive units

while BTA-amine and Jeffamine-based side-chains were applied to ensure the formation of compartmentalized, water-soluble SCPNs. P7 was then prepared to extend the application potential of the SCPN-based platform. P7, which is otherwise identical to P6, was additionally functionalized with coumarin units through a $^1\text{O}_2$ -cleavable amino-acrylate linker.²⁴ The coumarin unit is a mimic for a prodrug model and site-specific “drug” activation and release can be triggered by a cascade of $^1\text{O}_2$ generation and subsequent cleavage of the $^1\text{O}_2$ -cleavable linker.²⁵ The pPFPA₁₅₀ was first modified with BTA-amine, 4-(2-amino-ethyl)-piperidine-1-carboxylic acid *tert*-butyl ester and Jeffamine, then with Boc-group deprotection to obtain polymers with piperidine groups. The final polymers were obtained by further coupling of these piperidine-containing polymers with different ratio of carboxyl acid functionalized porphyrin derivative and alkyne-functionalized coumarin derivative. Reference polymers P8 (lacking the porphyrin moiety) and P9 (containing only BTA and Jeffamine) were also prepared.

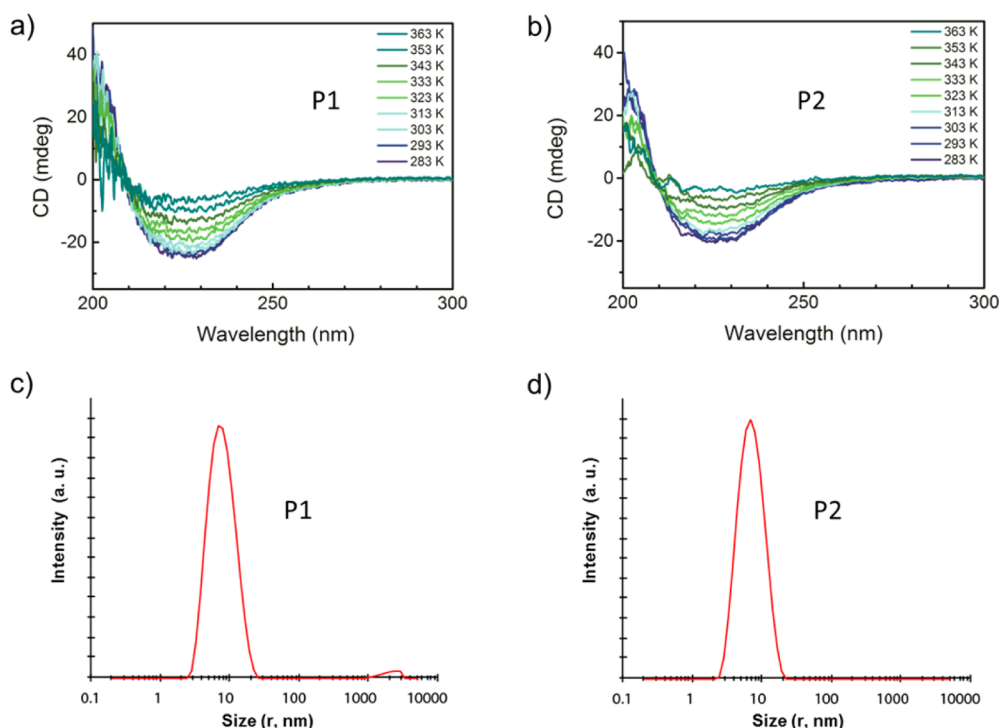


Figure 2. Temperature-dependent CD spectra from 283 to 363 K of (a) P1 and (b) P2 in water ($[BTA] = 50 \mu\text{M}$, optical path length = 0.5 cm). DLS measurements of (c) P1 (1.0 mg mL^{-1} , $R_h = 8.2 \text{ nm}$) and (d) P2 (1.0 mg mL^{-1} , $R_h = 7.4 \text{ nm}$) in water.

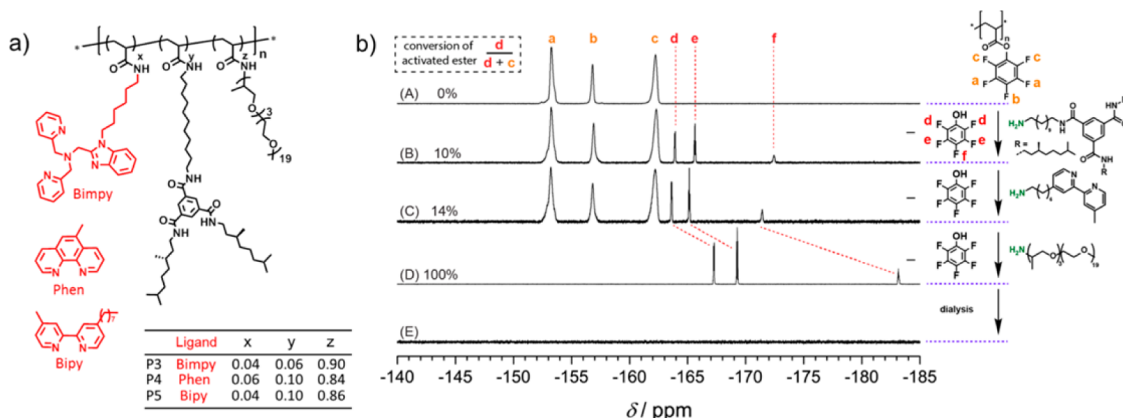


Figure 3. (a) Chemical structures of P3–P5; (b) ^{19}F NMR spectra in CDCl_3 of pPFPA $_{100}$ (A) and its sequential modification with BTA-NH $_2$ (B), Bipy-NH $_2$ (C), and Jeffamine (D) to prepare P5, which does not contain any ^{19}F after dialysis (E).

The characterization by SEC and DLS of P3–P9 is summarized in Table 2. Note that the polymers are derived from different precursor polymers (pPFPA $_{100}$, pPFPA $_{150}$, pPFPA $_{170}$) and hence show differences in their degrees of polymerization (DPs). By comparing the CD spectra and DLS results of P3–P5 with those of P1 and P2, we conclude that the introduction of ligands does not significantly affect the single-chain folding behavior of the polymers; all form SCPNs in aqueous solution with an ordered inner structure (Figures S7, S9). Moreover, P6, which contains 2% porphyrin, 9% BTAs and 89% Jeffamine-based units, shows excellent solubility in water. The presence of porphyrin is indicated by the red color of the solution, and the porphyrin concentration can reach up to $200 \mu\text{M}$. Both CD and DLS measurements of P6 confirmed that single-chain folding behavior occurs (Figures S8, S9). From the combined CD and DLS results we concluded that these novel amphiphilic polyacrylamides behave similar to our previously

reported polymethacrylates.^{3d–g} Neither the presence of ligands and porphyrin nor the amide-based polymeric backbone negatively affects the single-chain folding of the polymers into SCPNs.

Ligand-Containing SCPNs as Organometallic Catalysts. The catalytic activity of P3 and P4, which contain Bimpy and Phen ligands, in CuAAC reactions was studied first. As a model reaction, 3-azido-7-hydroxycoumarin and propargyl alcohol were chosen as azide and alkyne substrates. The azidocoumarin is nonfluorescent, and the lone pair of electrons from the azido moiety quenches the fluorescence of the coumarin moiety.^{7e} After forming the triazole ring, the lone pair of electrons are localized thus activating the fluorescence (Figure 5a). By using fluorescence as a “turn-on” property, the kinetics of the CuAAC reactions with different catalysts can easily be monitored by fluorescence spectroscopy.²⁶ We performed the CuAAC reactions at dilute substrate conditions

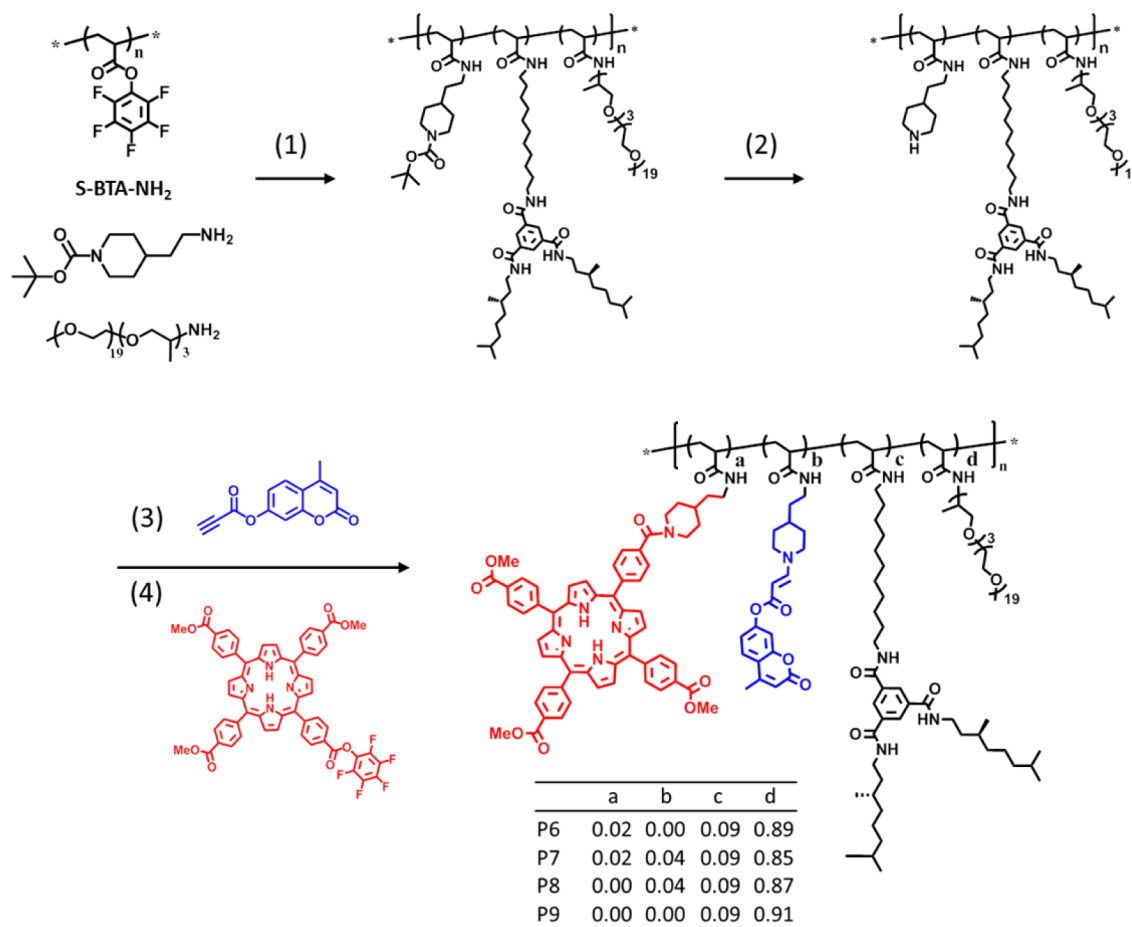


Figure 4. Synthesis of polymers P6–P9. (1) Sequential modification of pPFPA₁₅₀ with the amines, THF, 50 °C; (2) trifluoroacetic acid, RT; (3) THF, RT; (4) THF, 50 °C.

Table 2. Characterization of Polymers pPFPA₁₅₀, pPFPA₁₇₀, and P3–P9 by SEC and DLS

polymer	$M_{n,SEC}$ [kDa] ^a	\bar{D} [–] ^a	R_h [nm] ^d	DP [–] ^b	$M_{n,ca}$ [kDa] ^c
pPFPA ₁₅₀	20.6	1.18		150	36.0
pPFPA ₁₇₀	23.7	1.30		170	40.7
P3	39.4	1.58	9.6	170	178.2
P4	32.8	1.47	10.2	150	151.0
P5	27.4	1.42	8.9	100	102.7
P6	39.7	1.31	8.6	150	158.8
P7	37.1	1.47	11.4	150	154.7
P8	37.0	1.29	10.5	150	155.0
P9	34.1	1.23	11.6	150	159.2

^apPFPA₁₅₀ and pPFPA₁₇₀ were measured in THF, relative to polystyrene standards; P3–P9 were measured in DMF with 10 mM LiBr, relative to poly(ethylene oxide) standards. ^bThe degree of polymerization (DP) was calculated from the monomer PFPA conversion by NMR to prepare precursor polymer pPFPA. ^cCalculated molecular weight derived from the DP. ^dHydrodynamic radius as determined by DLS.

([azidocoumarin] = 80 μ M and [propargyl alcohol] = 200 μ M) using CuSO₄ (40 μ M) and sodium ascorbate (NaAsc, 2 mM) to generate Cu(I) in situ. Then, P3 or P4 were added with a ligand:Cu ratio of 1:1 for Bimpy and 2:1 for Phen. All experiments were performed in phosphate buffer (0.01 M) with 2% DMSO at a physiological pH of around 7.4. Fluorescence-time curves of the P3@Cu(I), P4@Cu(I), and Cu(I) catalyzed

CuAAC reactions are shown in Figure 3b. P3 with Bimpy as Cu(I)-binding ligand shows the most effective catalysis of CuAAC reaction—the fluorescence reaches a plateau within less than 10 min. By employing liquid chromatography–mass spectrometry (LC–MS), we confirmed that the fluorescence intensity reaches a plateau that corresponds to full conversion of azidocoumarin into triazole coumarin (Figure S10). In the case of P4 with Phen ligands, the reaction also proceeded rapidly and was completed in about 25 min. In contrast, in the absence of ligands, the reaction with only Cu(I) was much slower.

Pd-based catalysts are another powerful tool in organic synthesis and, compared to copper, they are more biologically inert.¹⁰ To evaluate our SCPN-supported Pd-based catalyst, an *N*-propargyloxycarbonyl-caged rhodamine **1** was chosen as fluorogenic reporter.^{10b–d} While **1** itself is virtually non-fluorescent, cleavage of one propargyl group results in the fluorescent product **2** and full “decaging” results in highly fluorescent **3**. P5 (1.5 mg mL^{−1}, [Bipy] = 60 μ M, in PBS buffer) was loaded with Pd(OAc)₂ (50 μ M) to form P5@Pd(II) catalyst. Substrate **1** was dissolved in DMSO and was added to a P5@Pd(II) solution with a final concentration of 50 μ M (in 98% PBS/2% DMSO). Kinetic curves of a solution of **1** with and without P5@Pd(II) catalyst were obtained by recording the increase in fluorescence signals (Figure S11). The fluorescence of the reaction mixture in the presence of P5@Pd(II) catalyst shows a much sharper increase in intensity than that without the catalyst, and nearly reaches a plateau after

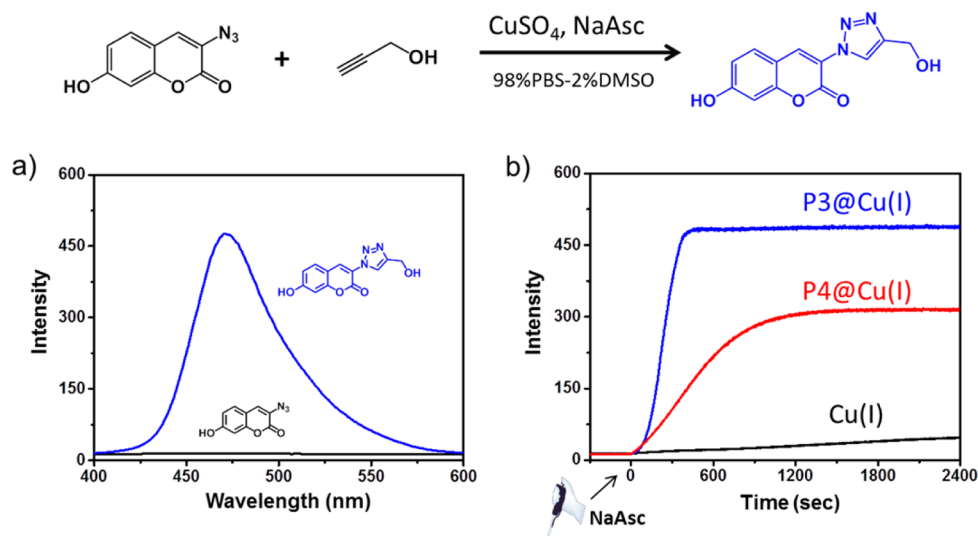


Figure 5. Model CuAAC reaction using 3-azido-7-coumarin and propargyl alcohol as substrates (3-azido-7-hydroxycoumarin 80 μM ; propargyl alcohol 200 μM ; P3 1.0 mg/mL, [Bimpy] = 40 μM ; P4 1.3 mg/mL, [Phen] = 80 μM ; CuSO₄ 40 μM ; NaAsc 2 mM). (a) Fluorescence of azidocoumarin before (black) and after (blue) the CuAAC reaction, λ_{ex} = 340 nm. (b) Fluorescence-time curve of P3@Cu(I) (blue), P4@Cu(I) (red), and Cu(I) (black), λ_{ex} = 340 nm, recorded at λ_{em} = 470 nm.

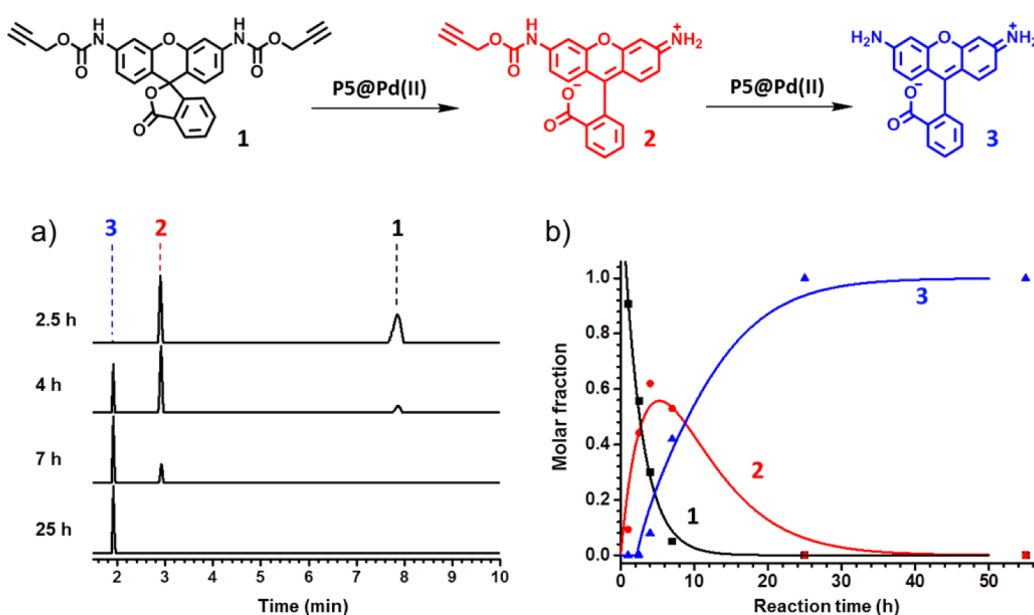


Figure 6. P5@Pd(II) catalyzed depropargylation reaction of a *N*-propargyloxycarbonyl-caged rhodamine (P5 1.5 mg mL⁻¹, [Bipy] = 60 μM ; Pd(OAc)₂ = 50 μM , [1] = 50 μM). (a) LC-MS traces of 1 solution with P5@Pd(II) catalyst at different reaction times, monitored with UV detection. (b) Composition of the reaction mixture at different reaction times based on LC-MS measurements.

around 25 h (Figure S11). LC-MS was employed to obtain more quantitative information on the conversion of 1 into 3. The composition of the reaction mixture at different time points was estimated from the LC-MS data and the molar extinction coefficients ϵ .²⁷ As shown in Figure 6, 1 undergoes a two-step depropargylation process and the reaction is completed within 25 h in the presence of P5@Pd(II) catalyst. Without catalyst, less than 10% of 3 could be detected even after more than 70 h.

Porphyrin-Containing SCPNs as Modular Platform toward Photosensitizer Drugs. We hypothesized that SCPN-based photosensitizers would have several novel features compared to existing systems: (i) the compartmented hydrophobic interior of SCPNs can accommodate the photosensitizer

units and isolate them to prevent aggregation; (ii) the oEG-based exterior of SCPNs is anticipated to provide the porphyrin-containing SCPNs not only with good water-solubility but also with longevity in the blood circulation; (iii) the SCPNs possess an intact but still rather open structure, which allows the generated ROS to diffuse out of the SCPNs; (iv) the synthetic polymer-based system holds great potential for further expansion to serve as a modular platform for additional function-integration, so that multifunctional photosensitizer drugs can be prepared.

We selected P6–P9 to assess the feasibility of SCPNs in photosensitization. First, the ability to generate ¹O₂ by porphyrin-containing P6 was evaluated. UV-vis spectroscopy was employed to study the aggregation state of porphyrin

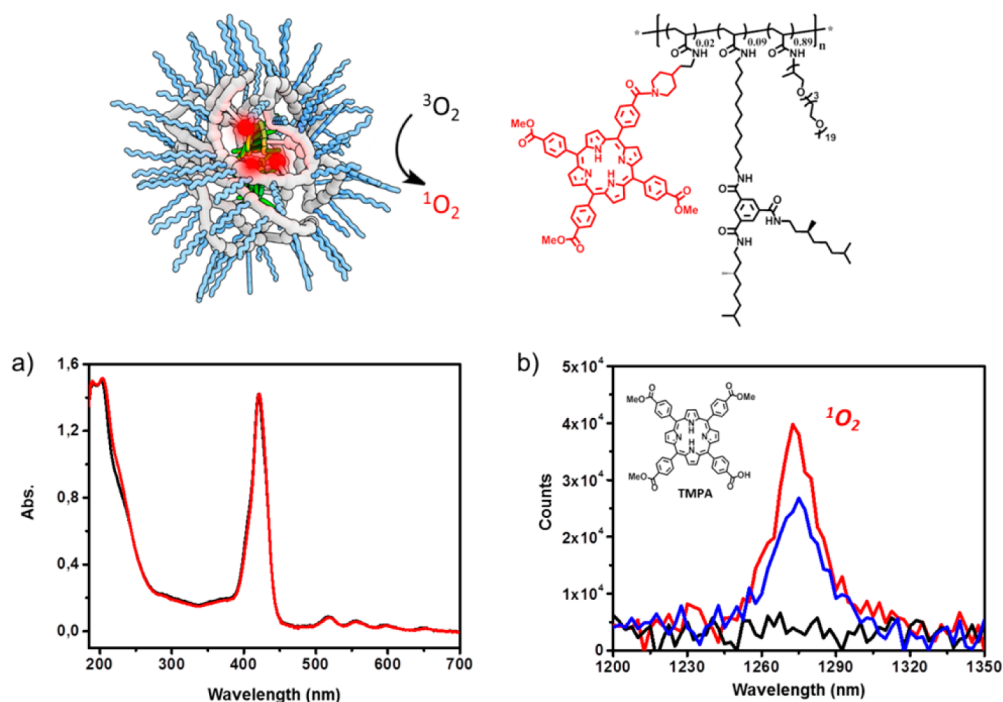


Figure 7. (a) UV-vis spectra of P6 (0.5 mg mL^{-1} in H_2O) at 10°C (black) and 90°C (red); (b) infrared emission spectra of P6 (0.5 mg mL^{-1} , [porphyrin] = $10 \mu\text{M}$, red), TMPA ($10 \mu\text{M}$, black), and P9@TMPA (P9 at 0.5 mg mL^{-1} , [TMPA] = $10 \mu\text{M}$, blue) in D_2O , $\lambda_{\text{ex}} = 420 \text{ nm}$.

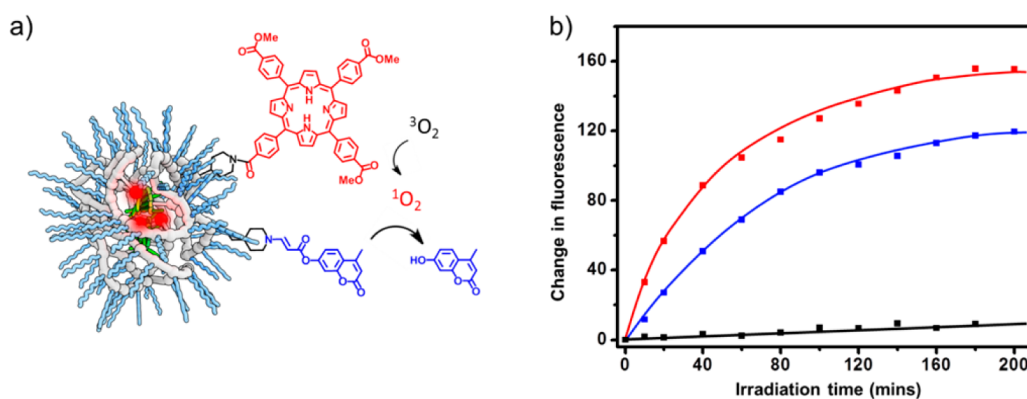


Figure 8. (a) Schematic illustration of the cascade of $^1\text{O}_2$ generation and pro-drug activation. (b) Fluorescence-time plot obtained from irradiation of P7 (red, 1.0 mg mL^{-1}), P8 (black, 1.0 mg mL^{-1}), and P6/P8 (blue, both P6 and P8 are at 1.0 mg mL^{-1}) ($\lambda_{\text{ex}} = 320 \text{ nm}$, $\lambda_{\text{em}} = 455 \text{ nm}$).

moieties in the SCPNs. The absorption spectra of P6 are shown in Figure 7a. The characteristic Soret band of porphyrin appeared as a sharp peak at 420 nm and highly similar to the absorption of molecularly dissolved porphyrins in organic solvents. Additionally, the absorption of P6 showed no shift upon increasing the temperature up to 90°C , suggesting that the porphyrins in the SCPNs were not aggregated and remained in their monomeric form.

To test the $^1\text{O}_2$ generation ability of P6 in solution, the luminescence of $^1\text{O}_2$ was directly investigated by infrared emission spectroscopy (IRES).²⁸ As shown in Figure 7b, a strong characteristic emission of $^1\text{O}_2$ at 1275 nm was observed after excitation of the P6 solution at 420 nm . 4-(10,15,20-tris(4-(methoxycarbonyl)phenyl)porphyrin-5-yl)benzoic acid (TMPA), which has a porphyrin structure similar to P6 but without SCPN support, was also tested. In contrast to P6, TMPA forms an almost colorless solution with purple-black precipitates due to its poor water solubility. The mixture was measured by IRES and the $^1\text{O}_2$ signal was virtually absent.

Interestingly, the addition of P9 to the mixture resulted in partial dissolving of the TMPA precipitates and the formation of a colored solution. In this case, emission of $^1\text{O}_2$ was detected with P9-TMPA solution. The results above show that the SCPNs act as water-soluble carriers for porphyrins and prevent porphyrin moieties from aggregating, thus permitting the generation of $^1\text{O}_2$.

P7, designed to function as a multifunctional SCPN-based photosensitizer drug, can also produce $^1\text{O}_2$ by photoirradiation, and the released $^1\text{O}_2$ can cleave the amino-acrylate linker connecting the coumarin moiety and the polymer backbone. The fluorescence of coumarin moieties is quenched in the presence of amino-acrylate linkers and can be “turned on” after cleavage of the linkers. The pro-drug model activation experiment was performed by photoirradiation of the P7 solution with a halogen lamp. The fluorescence intensity was measured at different irradiation times from 0 to 200 min. As shown in Figure 8, the fluorescence of the P7 solution increased significantly upon photoirradiation, indicating that the cascade

activation of the prodrug works. In contrast, the P8 solution, which contains coumarin moieties but no porphyrins, shows almost no change in fluorescence intensity, which suggests that the amino-acrylate linkers themselves are stable under photoirradiation. P6, which contains porphyrins, was then mixed with P8 solution and irradiated. The fluorescence increased, which means that the $^1\text{O}_2$ produced by P6 can also activate the prodrug in P8. This nicely illustrates that the $^1\text{O}_2$ produced in P6 can easily diffuse out, indicating that the SCPN's structure is relatively open.

CONCLUSION

In conclusion, a modular approach using the postpolymerization modification of pPFPA is a rapid and convenient way to access well-defined, functional copolymers that form water-soluble SCPNs as a result of the helical self-assembly of the pendant BTA motifs. Ligand-containing SCPNs, capable of binding to Cu(I) or Pd(II), were prepared for bio-orthogonal organometallic catalysts while porphyrin-containing SCPNs were prepared to investigate the potential of SCPNs as photosensitizers. All polymers folded in compact conformations in water, and the presence of ligands or porphyrins did not negatively affect their folding behavior. The SCPNs comprising Cu(I) significantly accelerated azide-alkyne cycloaddition reactions while SCPNs ligated to Pd(II) efficiently catalyze depropargylation reactions. These catalytic reactions proceeded efficiently in phosphate buffer at a physiological pH and at low substrate concentrations. In addition, the porphyrin-containing SCPNs produced singlet oxygen ($^1\text{O}_2$) upon photoirradiation. Moreover, by attaching both porphyrins and prodrug models, attached via $^1\text{O}_2$ -cleavable amino-acrylate linker, to the SCPNs, the irradiation of the SCPNs resulted in a cascade reaction of $^1\text{O}_2$ generation followed by cleavage of the amino-acrylate linkers, releasing the drug model. The modular synthesis strategy reported here provides rapid and controlled access to SCPNs with tunable amounts of active units that fulfill different functions. Our current efforts are directed toward the application of these systems in complex media, for example, cellular environments, where site isolation and control over the three-dimensional structure is crucial for activity.

ASSOCIATED CONTENT

Supporting Information

The Supporting Information is available free of charge on the ACS Publications website at DOI: 10.1021/jacs.5b08299.

Experimental and synthetic details, CD spectra, DLS, and ^1H NMR spectra (PDF)

AUTHOR INFORMATION

Corresponding Authors

*a.palmans@tue.nl

*e.w.meijer@tue.nl

Author Contributions

[†]Y.L. and T.P. contributed equally to the work.

Notes

The authors declare no competing financial interest.

ACKNOWLEDGMENTS

T.P. thanks the German Academic Exchange Service for financial support via a DAAD Research Fellowship for Postdoctoral Researchers. Y.L., S.P., A.R.A.P., and E.W.M.

acknowledge financial support from the Dutch Ministry of Education, Culture and Science (Gravity program 024.001.035) and the European Research Council (FP7/2007-2013, ERC Grant Agreement 246829). The ICMS animation studio is acknowledged for providing the artwork.

REFERENCES

- (1) (a) Astruc, D.; Chardac, F. *Chem. Rev.* **2001**, *101*, 2991–3024. (b) Deraedt, C.; Pinaud, N.; Astruc, D. *J. Am. Chem. Soc.* **2014**, *136*, 12092–12098. (c) Zimmerman, S. C.; Wendland, M. S.; Rakow, N. A.; Zharov, I.; Suslick, K. S. *Nature* **2002**, *418*, 399–403. (d) Astruc, D. *Nat. Chem.* **2012**, *4*, 255–267. (e) Bosman, A. W.; Heumann, A.; Klaerner, G.; Benoit, D.; Fréchet, J. M. J.; Hawker, C. J. *J. Am. Chem. Soc.* **2001**, *123*, 6461–6462. (f) Helms, B.; Meijer, E. W. *Science* **2006**, *313*, 929–930. (g) Yashima, E.; Maeda, K.; Iida, H.; Furusho, Y.; Nagai, K. *Chem. Rev.* **2009**, *109*, 6102–6211. (h) Yamamoto, T.; Yamada, T.; Nagata, Y.; Sugimoto, M. *J. Am. Chem. Soc.* **2010**, *132*, 7899–7901. (i) Guichard, G.; Huc, I. *Chem. Commun.* **2011**, *47*, 5933–5941. (j) Adronov, A.; Fréchet, J. M. J. *Chem. Commun.* **2000**, 1701–1710. (k) Rodionov, V. H.; Gao, S.; Scroggins; Unruh, D. A.; Avestro, A.-J.; Fréchet, J. M. J. *J. Am. Chem. Soc.* **2010**, *132*, 2570–2572. (l) Helms, B.; Guillaudeu, S. J.; Xie, Y.; McMurdo, M.; Hawker, C. J.; Fréchet, J. M. J. *Angew. Chem., Int. Ed.* **2005**, *44*, 6384–6387. (m) Zhang, X.; Xu, H.; Dong, Z.; Wang, Y.; Liu, J.; Shen, J. *J. Am. Chem. Soc.* **2004**, *126*, 10556–10557. (n) Yu, J.; RajanBabu, T. V.; Parquette, J. R. *J. Am. Chem. Soc.* **2008**, *130*, 7845–7847.
- (2) (a) Ouchi, M.; Badi, N.; Lutz, J.-F.; Sawamoto, M. *Nat. Chem.* **2011**, *3*, 917–924. (b) Harth, E.; van Horn, B.; Lee, Y. Y.; Germack, D. S.; Gonzales, C. P.; Miller, R. D.; Hawker, C. J. *J. Am. Chem. Soc.* **2002**, *124*, 8653–8660. (c) Beck, J. B.; Killips, K. L.; Kang, T.; Sivanandan, K.; Bayles, A.; Mackay, M. E.; Wooley, K. L.; Hawker, C. J. *Macromolecules* **2009**, *42*, 5629–5635. (d) Cherian, A. E.; Sun, F. C.; Sheiko, S. S.; Coates, G. W. *J. Am. Chem. Soc.* **2007**, *129*, 11350–11351. (e) Murray, B. S.; Fulton, D. A. *Macromolecules* **2011**, *44*, 7242–7252. (f) Appel, E. A.; Barrio, J. D.; Dyson, J.; Isaacs, L.; Scherman, O. A. *Chem. Sci.* **2012**, *3*, 2278–2281. (g) Pomposo, J. A. *Polym. Int.* **2014**, *63*, 589–592. (h) Altintas, O.; Barner-Kowollik, C. *Macromol. Rapid Commun.* **2012**, *33*, 958–971. (i) Gonzalez-Burgos, M.; Latorre-Sanchez, A.; Pomposo, J. A. *Chem. Soc. Rev.* **2015**, *44*, 6122–6142.
- (3) (a) Foster, E. J.; Berda, E. B.; Meijer, E. W. *J. Am. Chem. Soc.* **2009**, *131*, 6964–6966. (b) Mes, T.; van der Weegen, R.; Palmans, A. R. A.; Meijer, E. W. *Angew. Chem., Int. Ed.* **2011**, *50*, 5085–5089. (c) Hosono, N.; Gillissen, M. A. J.; Li, Y. C.; Sheiko, S. S.; Palmans, A. R. A.; Meijer, E. W. *J. Am. Chem. Soc.* **2013**, *135*, 501–510. (d) Terashima, T.; Mes, T.; De Greef, T. F. A.; Gillissen, M. A. J.; Besenius, P.; Palmans, A. R. A.; Meijer, E. W. *J. Am. Chem. Soc.* **2011**, *133*, 4742. (e) Huerta, E.; Stals, P. J. M.; Meijer, E. W.; Palmans, A. R. A. *Angew. Chem., Int. Ed.* **2013**, *52*, 2906–2910. (f) Artar, M.; Terashima, T.; Sawamoto, M.; Meijer, E. W.; Palmans, A. R. A. *J. Polym. Sci., Part A: Polym. Chem.* **2014**, *52*, 12–20. (g) Gillissen, M. A. J.; Terashima, T.; Meijer, E. W.; Palmans, A. R. A.; Voets, I. K. *Macromolecules* **2013**, *46*, 4120–4125. (h) Stals, P. J. M.; Gillissen, M. A. J.; Paffen, T. F. E.; de Greef, T. F. A.; Lindner, M. M.; Meijer, E. W.; Palmans, A. R. A.; Voets, I. K. *Macromolecules* **2014**, *47*, 2947–2954.
- (4) (a) Prescher, J. A.; Bertozzi, C. R. *Nat. Chem. Biol.* **2005**, *1*, 13–21. (b) Sletten, E. M.; Bertozzi, C. R. *Angew. Chem., Int. Ed.* **2009**, *48*, 6974–6998. (c) Streu, C.; Meggers, E. *Angew. Chem., Int. Ed.* **2006**, *45*, 5645–5648. (d) Sasmal, P. K.; Streu, K. N.; Meggers, E. *Chem. Commun.* **2013**, *49*, 1581–1587.
- (5) Dolmans, D. E. J. G. J.; Fukumura, D.; Jain, D. K. *Nat. Rev. Cancer* **2003**, *3*, 380–387.
- (6) (a) Rostovtsev, V. V.; Green, L. G.; Fokin, V. V.; Sharpless, K. B. *Angew. Chem., Int. Ed.* **2002**, *41*, 2596–2599. (b) Kolb, H. C.; Finn, M. G.; Sharpless, K. B. *Angew. Chem., Int. Ed.* **2001**, *40*, 2004–2021. (c) Moses, J. E.; Moorhouse, A. D. *Chem. Soc. Rev.* **2007**, *36*, 1249–1262.

- (7) (a) Beatty, K. E.; Xie, F.; Wang, Q.; Tirrell, D. A. *J. Am. Chem. Soc.* **2005**, *127*, 14150–14151. (b) Uttamapinant, C.; Tangpeerachaikul, A.; Grecian, S.; Clarke, S.; Singh, U.; Slade, P.; Gee, K. R.; Ting, A. Y. *Angew. Chem., Int. Ed.* **2012**, *51*, 5852–5856. (c) Jiang, H.; Zheng, T.; Lopez-Aguilar, A.; Feng, L.; Kopp, F.; Marlow, F. L.; Wu, P. *Bioconjugate Chem.* **2014**, *25*, 698–706. (d) Yang, M.; Jalloh, A. S.; Wei, W.; Zhao, J.; Wu, P.; Chen, P. R. *Nat. Commun.* **2014**, *5*, 4981–4990. (e) Besanceney-Webler, C.; Jiang, H.; Zheng, T.; Feng, L.; del Amo, D. S.; Wang, W.; Klivansky, L. M.; Marlow, F. L.; Liu, Y.; Wu, P. *Angew. Chem., Int. Ed.* **2011**, *50*, 8051–8056.
- (8) Rensing, C.; Grass, G. *FEMS Microbiol. Rev.* **2003**, *27*, 197–213.
- (9) (a) Macomber, L.; Imlay, J. A. *Proc. Natl. Acad. Sci. U. S. A.* **2009**, *106*, 8344–8349. (b) Chillappagari, S. *J. Bacteriol.* **2010**, *192*, 2512–2524.
- (10) (a) Li, N.; Lim, R. K. V.; Edwardraja, S.; Lin, Q. *J. Am. Chem. Soc.* **2011**, *133*, 15316–15319. (b) Yusop, R. M.; Unciti-Broceta, A.; Johansson, E. M. V.; Sanchez-Martin, R. M.; Bradley, M. *Nat. Chem.* **2011**, *3*, 241–245. (c) Weiss, J. T.; Dawson, J. C.; Macleod, K. G.; Rybski, W.; Fraser, C.; Torres-Sanchez, C.; Patton, E. E.; Bradley, M.; Carragher, N. O.; Unciti-Broceta, A. *Nat. Commun.* **2014**, *5*, 3277–3285. (d) Li, J.; Yu, J.; Zhao, J.; Wang, J.; Zheng, S.; Lin, S.; Chen, L.; Yang, M.; Jia, S.; Zhang, X.; Chen, P. R. *Nat. Chem.* **2014**, *6*, 352–361. (e) Wang, J.; Cheng, B.; Li, J.; Zhang, Z.; Hong, W.; Chen, X.; Chen, P. R. *Angew. Chem., Int. Ed.* **2015**, *54*, 5364–5368.
- (11) Allison, R. R.; Downie, G. H.; Cuenca, R.; Hu, X.-H.; Childs, C. J. H.; Sibata, C. H. *Photodiagn. Photodyn. Ther.* **2004**, *1*, 27–42.
- (12) (a) Fernandez, D. A.; Awruch, J.; Dicio, L. E. *Photochem. Photobiol.* **1996**, *63*, 784–792. (b) Liu, K.; Liu, Y.; Yao, Y.; Yuan, H.; Wang, S.; Wang, Z.; Zhang, X. *Angew. Chem.* **2013**, *125*, 8443–8447. (c) Jang, W.-D.; Nishiyama, N.; Zhang, G.-D.; Harada, A.; Jiang, D.-L.; Kawauchi, S.; Morimoto, Y.; Kikuchi, M.; Koyama, H.; Aida, T.; Kataoka, K. *Angew. Chem.* **2005**, *117*, 423–427.
- (13) (a) Solomon, E. I.; Sundaram, U. M.; Machonkin, T. E. *Chem. Rev.* **1996**, *96*, 2563–2605. (b) Holm, R. H.; Kennepohl, P.; Solomon, E. I. *Chem. Rev.* **1996**, *96*, 2239–2314.
- (14) (a) Hosono, N.; Palmans, A. R. A.; Meijer, E. W. *Chem. Commun.* **2014**, *50*, 7990–7993. (b) Hosono, N.; Stals, P. J. M.; Palmans, A. R. A.; Meijer, E. W. *Chem. - Asian J.* **2014**, *9*, 1099–1107.
- (15) (a) Theato, P. *J. Polym. Sci., Part A: Polym. Chem.* **2008**, *46*, 6677–6687. (b) Gunay, K. A.; Theato, P.; Klok, H.-A. *J. Polym. Sci., Part A: Polym. Chem.* **2013**, *51*, 1–28.
- (16) Schattling, P.; Jochum, F. D.; Theato, P. *Chem. Commun.* **2011**, *47*, 8859–8861.
- (17) Woodfield, P. A.; Zhu, Y.; Pei, Y.; Roth, P. J. *Macromolecules* **2014**, *47*, 750–762.
- (18) Arnold, R. M.; McNitt, C. D.; Popik, V. V.; Locklin, J. *Chem. Commun.* **2014**, *50*, 5307–5309.
- (19) (a) Eberhardt, M.; Mruk, R.; Zentel, R.; Theato, P. *Eur. Polym. J.* **2005**, *41*, 1569–1575. (b) Kakuchi, R.; Zamfir, M.; Lutz, J.-F.; Theato, P. *Macromol. Rapid Commun.* **2012**, *33*, 54–60. (c) Xu, L. Q.; Jiang, H.; Neoh, K.-G.; Kang, E.-T.; Fu, G. D. *Polym. Chem.* **2012**, *3*, 920–927. (d) Doncom, K. E. B.; Hansell, C. F.; Theato, P.; O'Reilly, R. K. *Polym. Chem.* **2012**, *3*, 3007–3015. (e) Moore, B. L.; O'Reilly, R. K. *J. Polym. Sci., Part A: Polym. Chem.* **2012**, *50*, 3567–3574. (f) Zamfir, M.; Theato, P.; Lutz, J.-F. *Polym. Chem.* **2012**, *3*, 1796–1802. (g) Roy, R. K.; Lutz, J.-F. *J. Am. Chem. Soc.* **2014**, *136*, 12888–12891.
- (20) (a) Presolski, S. I.; Hong, V.; Cho, S.-H.; Finn, M. G. *J. Am. Chem. Soc.* **2010**, *132*, 14570–14576. (b) Lewis, W. G.; Magallon, F. G.; Fokin, V. V.; Finn, M. G. *J. Am. Chem. Soc.* **2004**, *126*, 9152–9153.
- (21) Engle, K. M.; Yu, J.-Q. *J. Org. Chem.* **2013**, *78*, 8927–8955.
- (22) (a) Presolski, S. I.; Mamidyala, S. K.; Manzenrieder, F.; Finn, M. G. *ACS Comb. Sci.* **2012**, *14*, 527–530. (b) Schatzschneider, U.; Barton, J. K. *J. Am. Chem. Soc.* **2004**, *126*, 8630–8631.
- (23) Presolski, S. I.; van der Weegen, R.; Wiesfeld, J. J.; Meijer, E. W. *Org. Lett.* **2014**, *16*, 1864–1867.
- (24) (a) Bio, M.; Nkepan, G.; You, Y. *Chem. Commun.* **2012**, *48*, 6517–6519. (b) Bio, M.; Rajaputra, P.; Nkepan, G.; Awuah, S. G.; Hossion, A. M. L.; You, Y. *J. Med. Chem.* **2013**, *56*, 3936–3942.
- (25) Alvarez-Lorenzo, C.; Bromberg, L.; Concheiro, A. *Photochem. Photobiol.* **2009**, *85*, 848–860.
- (26) (a) Sivakumar, K.; Xie, F.; Cash, B. M.; Long, S.; Barnhill, H. N.; Wang, Q. *Org. Lett.* **2004**, *6*, 4603–4606. (b) Soriano Del Amo, D.; Wang, W.; Jiang, H.; Besanceney, C.; Yan, A. C.; Levy, M.; Liu, Y.; Marlow, F. L.; Wu, P. *J. Am. Chem. Soc.* **2010**, *132*, 16893–16899. (c) Presolski, S. I.; Hong, V. P.; Finn, M. G. *Curr. Protoc. Chem. Biol.* **2011**, *3*, 153–162.
- (27) (a) Lavis, L. D.; Chao, T.-Y.; Raines, R. T. *ACS Chem. Biol.* **2006**, *1*, 252–260. (b) Cai, S. X.; Zhang, H.-Z.; Guastella, J.; Drewe, J.; Yang, W.; Weber, E. *Bioorg. Med. Chem. Lett.* **2001**, *11*, 39–42.
- (28) Khan, A. U.; Kasha, M. *Proc. Natl. Acad. Sci. U. S. A.* **1979**, *76*, 6047–6049.